WSRC-RP-89-970

ALUMINUM-LITHIUM TARGET BEHAVIOR (U)

OCTOBER 1989

Westinghouse Savannah River Company
Savannah River Site
Aiken, SC 29808

SAFETY • RESPONSIBILITY • SECURITY
SRS
SAVANNAH RIVER SITE

PREPARED FOR THE U.S. DEPARTMENT OF ENERGY UNDER CONTRACT DE-AC09-88SR18035

WSRC-RP-89-970

Keywords:
Aluminum-Lithium Alloys
Tritium Production
Reactor target Materials

ALUMINUM-LITHIUM TARGET BEHAVIOR (U)

Authors:

W. R. McDONELL

Approved by:

E. L. Albenesius
Manager, Waste Technology Coordination

R. W. Benjamin
Manager, Operational Planning

Publication Date: October 1989

Westinghouse Savannah River Company
Savannah River Site
Aiken, SC 29808

ABSTRACT

Information on physical properties and irradiation behavior of aluminum-lithium target alloys employed for the production of tritium in Savannah River reactors has been reviewed to support development of technology for the New Production Reactor (NPR). Phase compositions and microstructures, thermal conductivity, mechanical properties, and constituent diffusion phenomena of the alloys, established in prior site studies, are presented. Irradiation behavior, including distributions of product tritium and helium and related exposure limits due to swelling and cracking of the target alloys is discussed, along with gas release processes occurring during subsequent product recovery operations.

The property review supports designation of the aluminum-lithium alloys as ideally well-suited target materials for low-temperature, tritium-producing reactors, demonstrated over 35 years of Savannah River reactor operation. Low temperature irradiation and reaction with lithium in the alloy promotes tritium retention during reactor exposure, and the aluminum provides a matrix from which the product is readily recovered on heating following irradiation.

CONTENTS

LIST OF FIGURES

LIST OF TABLES

ALUMINUM-LITHIUM TARGET BEHAVIOR

A. Introduction

Aluminum-lithium alloys are employed as target materials in SRS reactors for production of tritium (^3H) in accord with the following reaction:[1]

$$^6Li + n \rightarrow {}^3H + {}^4He$$

Neutrons from fission reactions in driver fuels are captured in Li-6 to produce tritium (^3H) in conjunction with the inert gas helium-4. Lithium content of the alloys has ranged generally 3 to 7-1/2 wt %, with the lithium initially of natural isotopic composition (7-1/2% Li-6), but in later applications specially enriched in the neutron absorbing isotope. Typical target alloys contain 3.2 wt % lithium, 50% enriched in Li-6, and are exposed in reactors to produce 100-1000 ppm tritium. Standard target types include control rods and slugs with 2-3 cm diameters and tubular elements typically either 4 cm or 9 cm diameter with various wall thicknesses. Properties and irradiation behavior of the Al-Li targets depend on alloy composition and structure as well as on reactor exposure conditions. Material specifications and irradiation conditions are prescribed to prevent dimensional instability during irradiation and minimize tritium release prior to product recovery.

B. Phase Compositions and Structures

The phase diagram for the Al-Li system shows a LiAl (β) phase of composition 20 wt % (50 wt %) lithium formed in the α-phase aluminum matrix (Figure B1).[2-4] The eutectic melting temperature is about 600°C. Solid solubility limits above which the LiAl phase forms are dependent on temperature as follows (Figure B2):[3-6]

200°C	0.6 wt %	(6 at %)
400°C	2.0 wt %	(8.5 at %)
600°C	3.9 wt %	(13.7 at %)

Microstructures dependent on heat treatment are produced in the alloys in accord with these phase equilibria (Figure B3).[3] As extruded structures show longitudinal stringers of β-phase LiAl in the α-phase Al matrix, with particles sizes about 6.5 E-04cm. Solution quenched structures retain Li up to solubility limits in the matrix, while solution-quenched and aged structures exhibit rod-shaped β-phase particles in the α-matrix.[4]

FIGURE B1

ALUMINUM-LITHIUM PHASE DIAGRAM

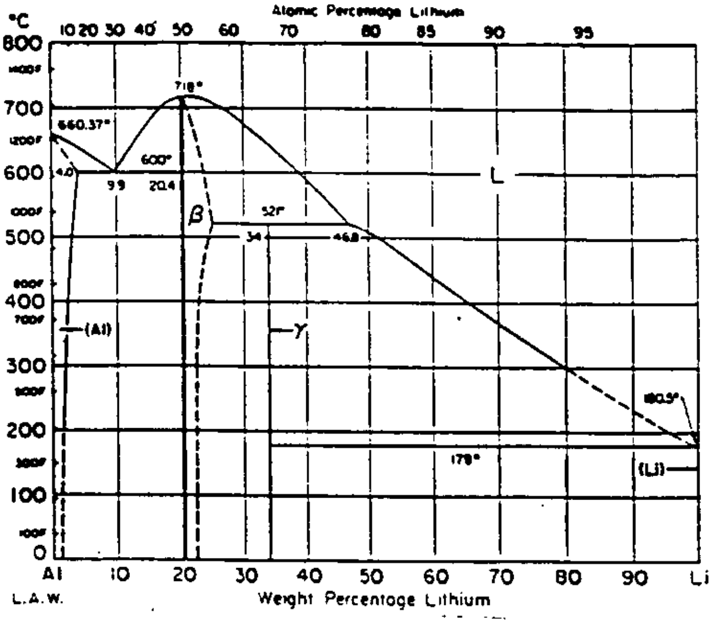

FIGURE B2

SOLID PHASE SOLUBILITY OF LITHIUM IN ALUMINUM

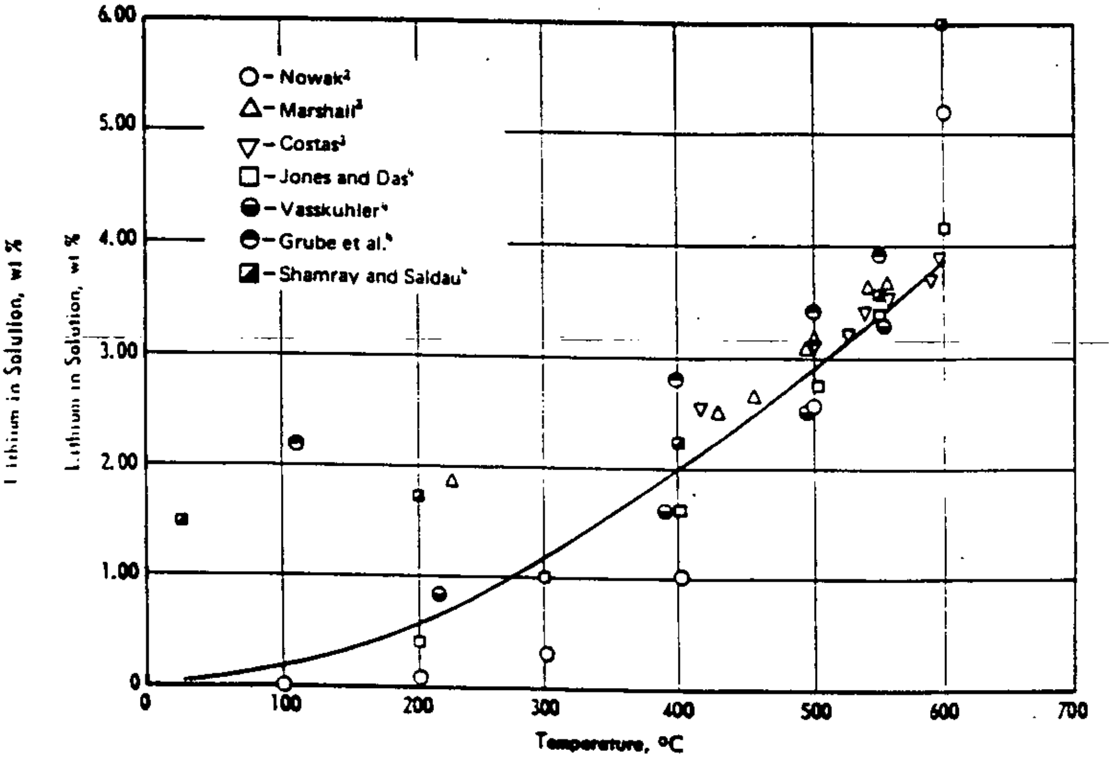

FIGURE B3

MICROSTRUCTURES OF ALUMINUM-LITHIUM ALLOYS

Neg. 14361 150X

A. As-Extruded

Neg. 17063 500X

B. Solution-Quenched

C. Thermal Conductivity

The addition of lithium to aluminum decreases thermal conductivity at approximately 150°C from 0.60 cal/(sec)(°C)(cm) at zero lithium content to 0.16 cal/(sec)(°C)(cm) for 7.9 wt % lithium (Table C1, Figure C1). The decrease in conductivity with increasing lithium addition is not uniform, however; the greatest decrease, from 0.60 to 0.22 cal/(sec)(°C)(cm), occurs on addition of the first 2 wt % lithium, whereas increasing the lithium content further linearly and more gradually decreases the conductivity to 0.16 cal/(sec)(°C) (cm) for a 7.9 wt % alloy. The rapid decline of conductivity in the 0 to 2 wt % lithium region is associated with the single-phase alloy, and the gradual and linear change beyond the 2 wt % content is attributed to the presence of β-phase LiAl compound.

The accuracy of the experimental values is believed to be at least ±10% and possibly ±5%.

TABLE C1

THERMAL CONDUCTIVITY DATA FOR ALUMINUM-LITHIUM ALLOYS

Metal, wt %	Thermal Conductivity, cal/(sec)(°C)(cm)	% Maximum Error	Temperature Range Employed, °C	Mean Temperature, °C
99.9+Al	0.599	4.6	107.7 - 146.8	127.2
	0.606	4.6	106.6 - 145.6	126.1
1.07 Li	0.329	2.1	158-7 - 235.8	196.7
	0.306	2.8	157.8 - 234.0	195.9
	0.307	2.7	119.7 - 194.7	157.2
1.40 Li	0.262	4.3	148.0 - 241.0	199.5
	0.266	3.1	150.8 - 240.5	195.7
2.30 Li	0.250[a]	2.6	155.2 - 214.9	185.0
	0.249[a]	2.6	155.2 - 214.9	185.0
	0.224	6.7	122.4 - 194.5	158.4
	0.218	4.2	188.2 - 321.9	255.1
	0.218	1.6	195.6 - 322.9	259.3
4.77 Li	0.189	2.9	142.8 - 219.5	181.1
	0.191	2.9	142.0 - 218.3	180.7
7.94 Li	0.158	2.5	135.5 - 217.7	176.6
	0.155	2.5	138.5 - 221.0	179.8

---

[a] Errors are suspected in the recording of original data.

FIGURE C1

THERMAL CONDUCTIVITY OF ALUMINUM-LITHIUM ALLOYS

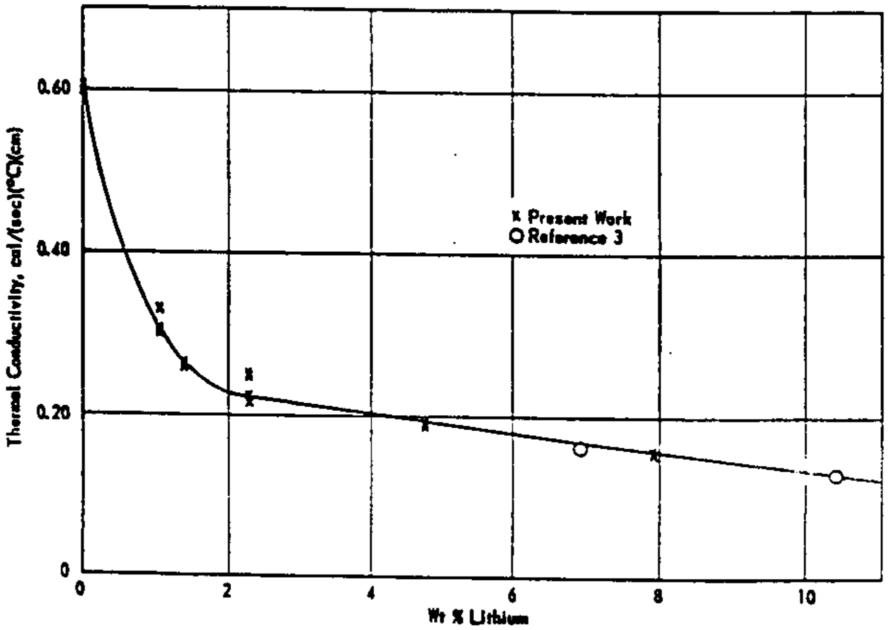

D. Lithium Diffusion

Isothermal.[8] Diffusivities of lithium in aluminum were measured over the range 400-600°C using diffusion couples of Al-LiAl produced by sealing metallic lithium inside thick walled Al cans (Table D1). Lithium concentration gradients were measured by microhardness profiles in metallographic sections through the capsules. Diffusivities were characterized by an activation energy E of 33.3 Kcal/mol and a diffusion factor D_0 of 4.5 cm^2sec (Figure D1).

Strain-Induced.[9] Straining of alloys containing >6 wt % Li during isothermal creep testing induces lithium diffusion and precipitation as LiAl on grain boundaries oriented 45° to 90° to the direction of applied stress (Figure D2). The thickness of the strain-induced precipitate layer in a binary two-phase Al-12 at % (3 wt %) Li alloy tested at temperatures 150-250°C increases with increasing strain. The strain-induced diffusion and precipitation are associated with structural changes at grain boundaries leading eventually to fracture.

Thermal Gradient.[10,11] Thermal gradients imposed on lithium-aluminum alloys induce lithium migration sufficient to cause significant distortion of target specimens during irradiation (Figure D3).[12] The lithium diffuses from hot to cold regions along α-phase grain boundary networks (Figure D4). Diffusion rates increase with increasing lithium content, and with increasing temperature and temperature gradients, with migration having negligible effect in alloys containing 1.5 and less wt % Li, or at temperatures less than 200°C (Table D2). Alloys in extruded and aged condition were least susceptible to migration, whereas solution quenched alloys were most susceptible and solution-treated and furnace-cooled or isothermally-aged alloys exhibited intermediate behavior.

FIGURE D1

ISOTHERMAL DIFFUSIVITY OF LITHIUM IN ALUMINUM

Diffusivity, D, was calculated from standard tables (2) that relate the ratio $(C-C_o)/(C_s-C_o)$ to $X\sqrt{Dt}$, where C is the concentration of lithium at X distance from the interface, C_S is the interface concentration, C_O is the initial lithium content of the aluminum, and t is the diffusion time. Since in this experiment C_O was zero, the ratio reduces to C/C_S. The distance, X, was 0.5 mm for all runs; C_S was the solubility limit at each temperature.

Temperature, °C	Duration of Run, hr	Diffusivity, cm²/sec
597	232	$1.5 - 2.8 \times 10^{-8}$
589	408	$1.7 - 2.8 \times 10^{-8}$
559	261	$5.5 - 10.0 \times 10^{-9}$
538	450	$2.2 - 8.6 \times 10^{-9}$
529	450	$4.2 - 5.2 \times 10^{-9}$
500	502	$2.0 - 2.8 \times 10^{-9}$
417	1020	$1.2 - 1.7 \times 10^{-10}$
310	2064	Not measurable

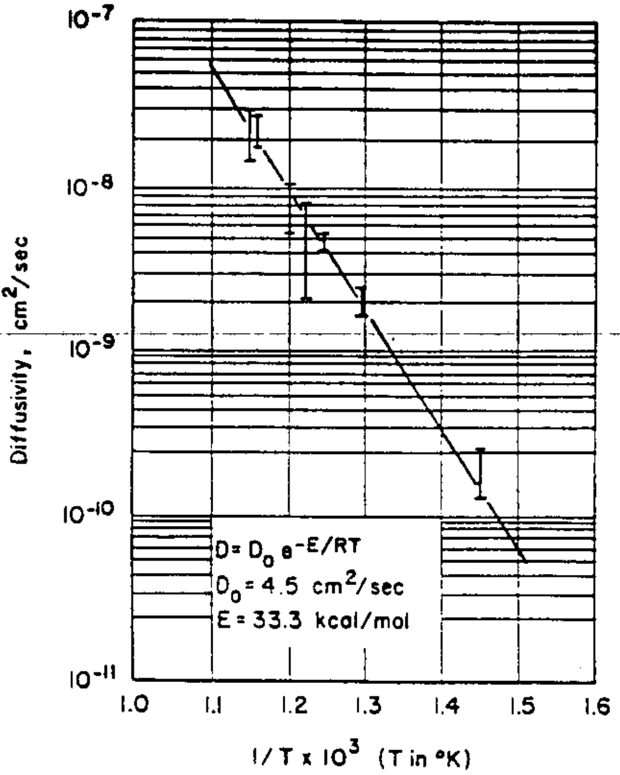

FIGURE D2

MICROSTRUCTURES SHOWING STRAIN-INDUCED DIFFUSION AND PRECIPITATION IN ALUMINUM-LITHIUM ALLOYS

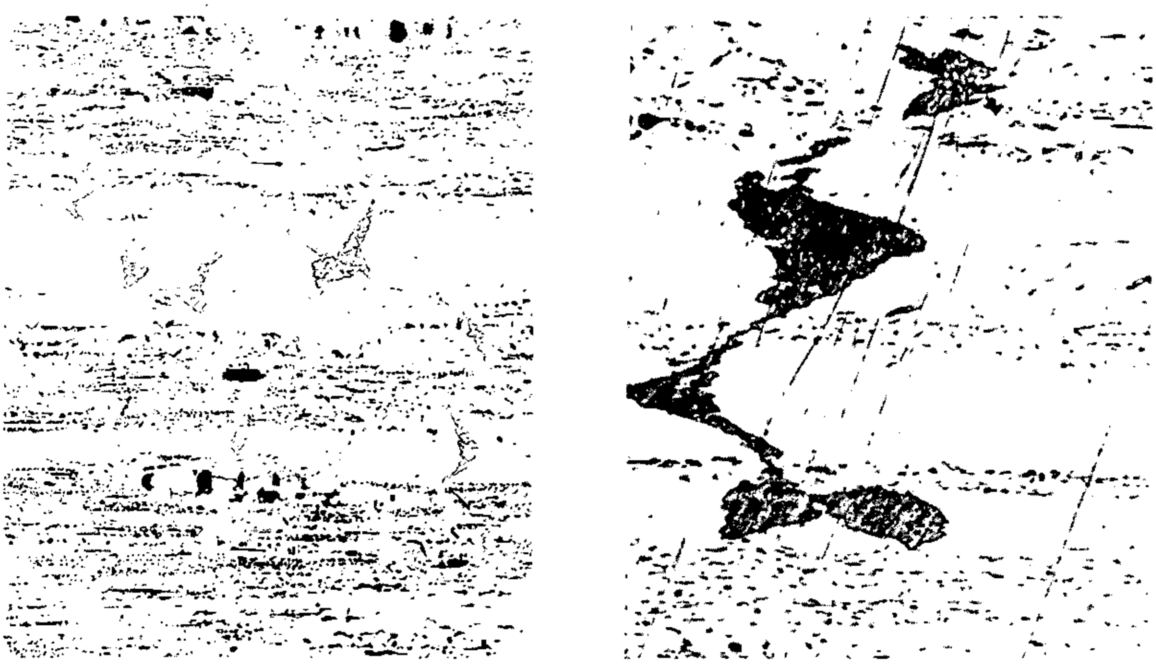

Neg. 27522 250X

A. Longitudinal, As-polished

Neg. 27257 500X

B. Longitudinal, As-polished, Slightly Oxidized in Air

FIGURE D3

DISTORTIONS CAUSED BY THERMAL GRADIENT DIFFUSION IN ALUMINUM-LITHIUM ALLOYS DURING IRRADIATION

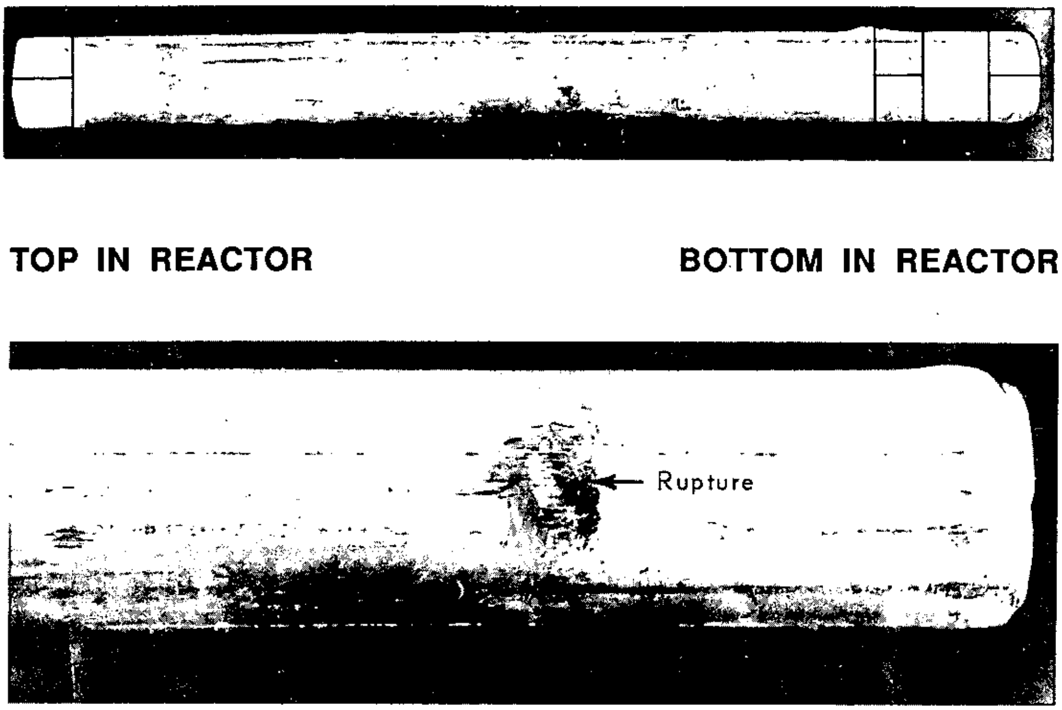

Bumps are areas of lithium diffusion to the core surface and into the can and sheath. Note cocked end cap and bulged sheath on bottom end of slug.

FIGURE D4

MICROSTRUCTURES OF ALUMINUM LITHIUM ALLOY IN THERMAL GRADIENT TEST

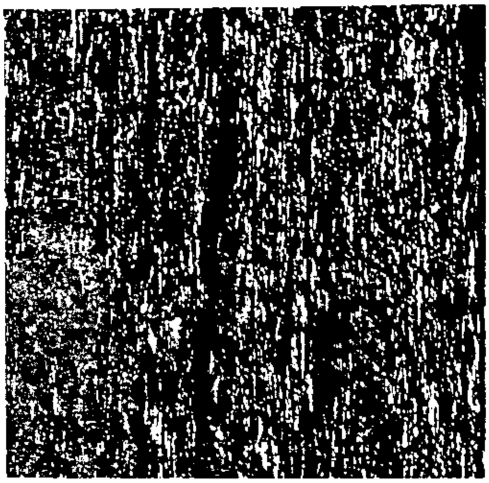

A. 14.7 wt % Li

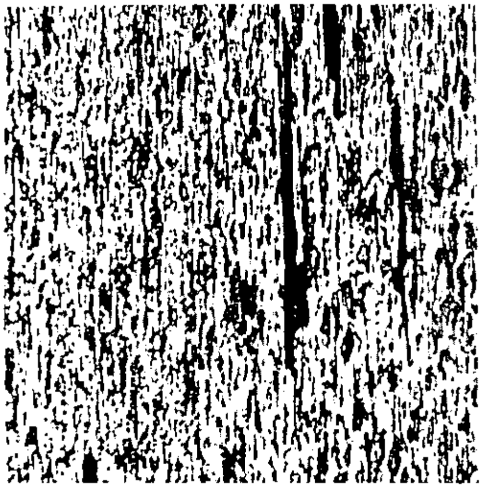

B. 7.7 wt % Li

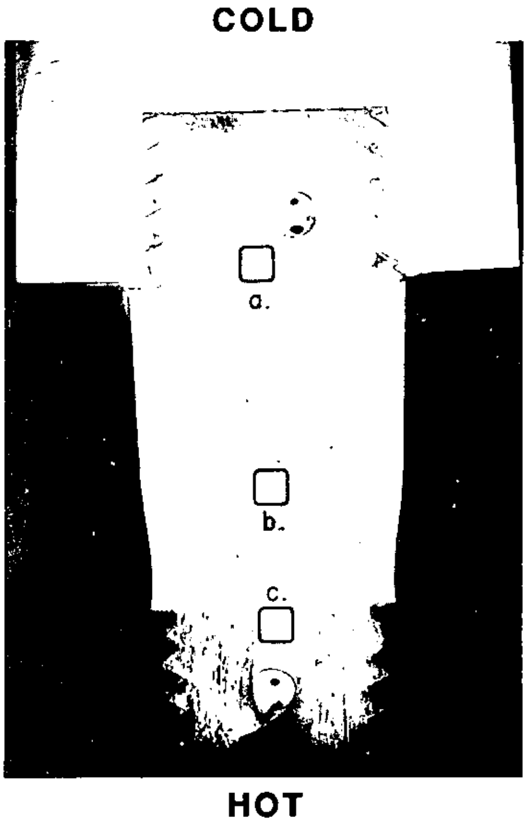

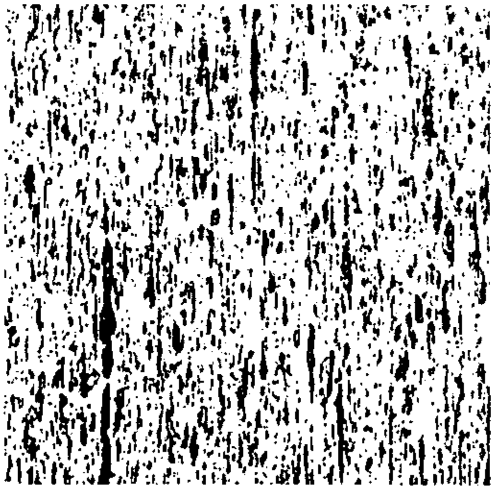

C. 2.8 wt % Li

This unirradiated 7.4 wt % specimen was in test for 840 hours with the hot end at 230°C. Note in the micrographs in A and B that the lithium concentration increased by the growth of a beta-phase network in the alpha grain boundaries (Micrographs 100X).

TABLE D1

EFFECT OF LITHIUM CONTENT ON THERMAL MIGRATION IN LITHIUM-ALUMINUM ALLOYS

WT % Li	Heat Treatment	Temperature, °C Hot	Temperature, °C Cold	Δ T/L, °C/Inch	Test Time	Amount of Migration
1.0	Solution-quenched[a]	414	300	98	283	None
1.5	Solution-quenched[a]	300	170	154	258	None
3.5	Extruded, then aged at 300°C for 24 hours	358	144	172	965	Very small
4.9	Solution-quenched[a]	310	126	145	269	Very large
4.9	Extruded, then aged at 300°C for 24 hours	314	123	150	269	Very large

---

[a] Solution heat-treated at 550°C, water-quenched

E. Mechanical Properties

Tensile-yield strengths and hardness of as-extruded Al-Li alloys containing up to 7.4 wt % lithium generally decrease with temperature and increase with lithium content (Table E1, Figures E1-E4). The mechanical properties of alloys containing up to 2 wt % lithium are not significantly affected by heat treatment, but for compositions containing 3 wt % lithium or more, as-extruded and aged specimens show higher strength than either solution quenched or dead annealed alloys.

Creep rates of a typical alloy (3.4 wt % Li) are sensitive to temperature and stress (Figure E5-E7), but insensitive to specimen heat treatment .[14] At higher stresses and temperatures, the alloy enters third stage creep directly from the first stage.

TABLE E1

MECHANICAL PROPERTIES OF 2.8 wt % AL-LI ALLOYS
(1/4-inch diameter specimens)

Alloy Condition	Tensile Strength (psi)	Yield Stress (psi)*	Prop. Limit (psi)	Elong- gation (%)	Area Reduction (%)	Modulus of Elasticity (psi)
		Room Temperature				
As-extruded	36,300	24,400	---	10.9	11.5	---
As-extruded + aged**	48,700	35,700	19,500	7.8	3.9	10.3
Furnace cooled+	36,500	28,400	20,600	3.1	3.1	9.6
Solution quenched, aged 1 hr 200°C	38,000	33,700	21,000	3.1	3.7	10.5
Solution quenched, aged 1 hr 300°C	19,640	14,550	7,450	40.0	62.0	5.7
Solution quenched++	18,560	13,990	10,920	47.0	50.0	12.0
		150°C				
As-extruded	28,100	21,400	14,550	10.9	16.0	9.9
As-extruded + aged**	37,000	36,500	28,500	9.4	13.4	7.6
Furnace cooled+	30,000	25,400	14,150	7.8	2.5	8.3
Solution quenched, aged 1 hr 200°C	30,800	---	---	0	0.8	---
Solution quenched, aged 1 hr 300°C	17,800	10,900	8,000	32.8	31.8	5.9
Solution quenched++	X	X	X	X	X	X
		250°C				
As-extruded	16,850	---	---	---	70	---
As-extruded + aged**	14,500	---	---	---	81.5	---
Furnace cooled+	14,590	---	---	---	24.4	---
Solution quenched, aged 1 hr 200°C	20,600	---	---	0	0	---
Solution quenched, aged 1 hr 300°C	X	X	X	X	X	X
Solution quenched++	17,300	---	---	---	1.6	---

* Yield stress based on 0.2% offset.
** Aging treatment consisted of 24 hours at 176°C.
\+ Furnace cooled from 550°C.
\++ Solution quenched from 570°C.

NOTE: The alloy composition of 2.8 w/o is a nominal value.
The above results were obtained from one tensile specimen only at each temperature and condition.
--- indicates data could not be obtained from specimen.
X indicates no sample run at that temperature and condition.

FIGURE E1

EFFECTS OF LITHIUM CONTENT ON TENSILE STRENGTH OF ALUMINUM-LITHIUM ALLOYS

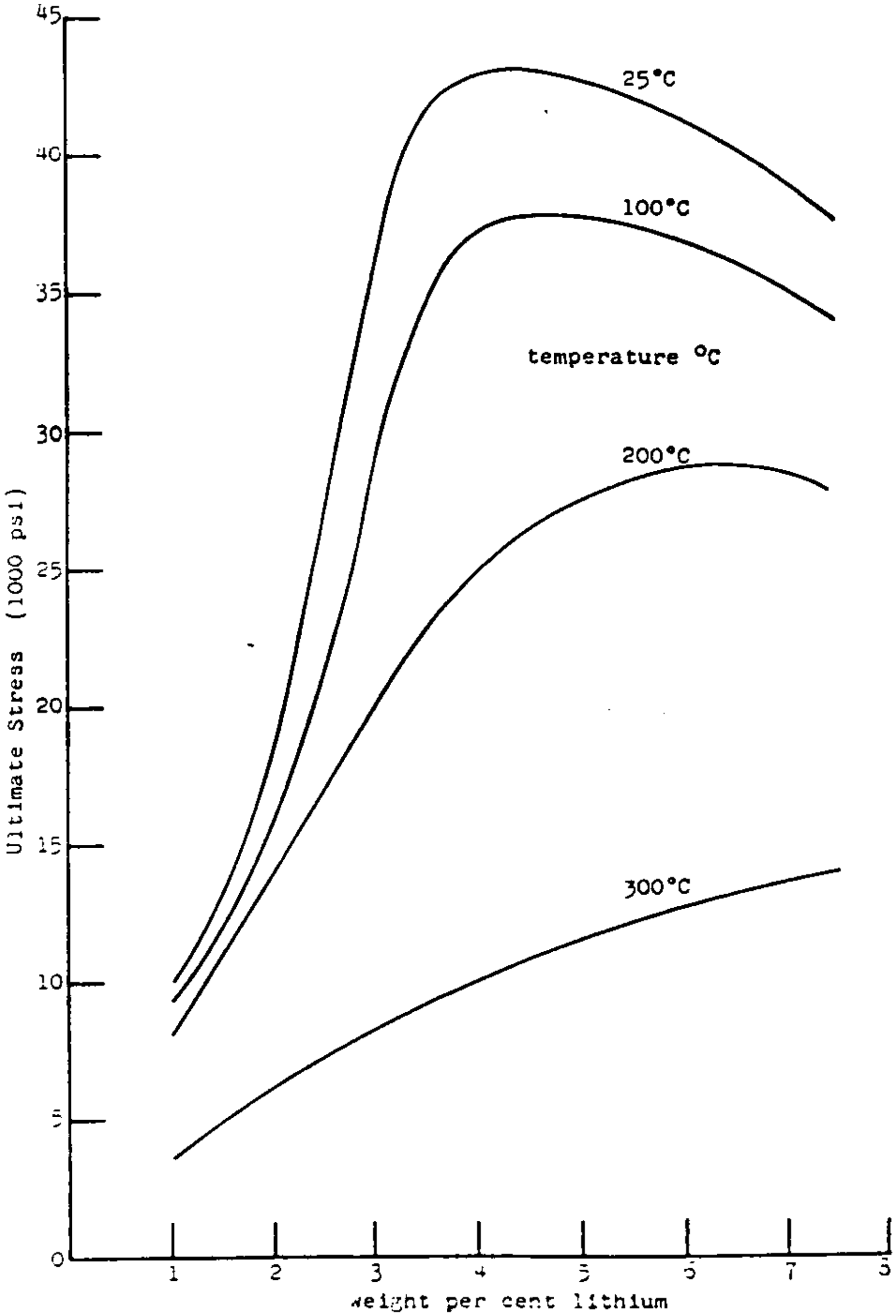

FIGURE E2

EFFECTS OF TEMPERATURE ON TENSILE STRENGTH OF ALUMINUM-LITHIUM ALLOYS

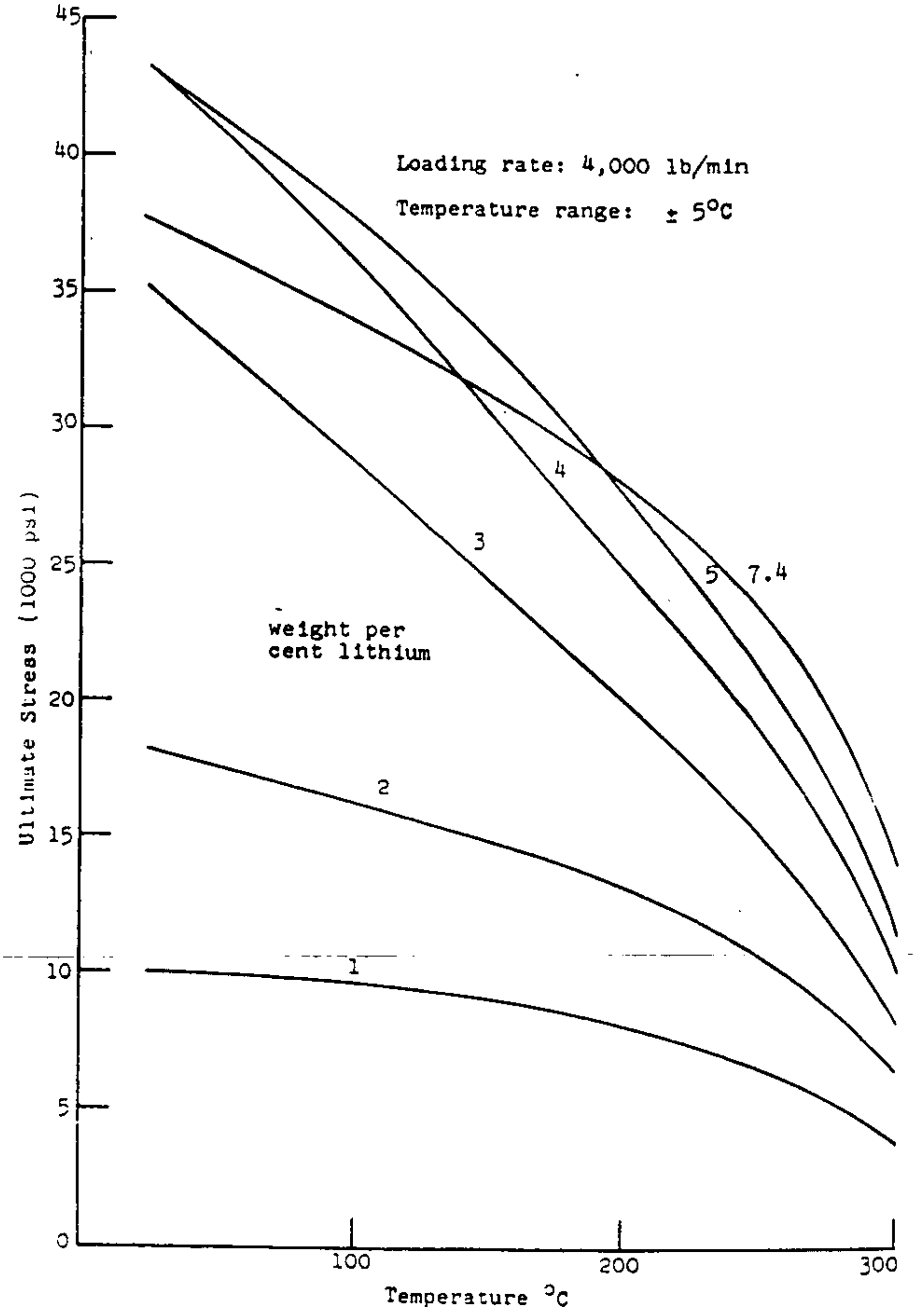

FIGURE E3

EFFECTS OF TEMPERATURE ON YIELD STRESS* OF ALUMINUM-LITHIUM ALLOYS

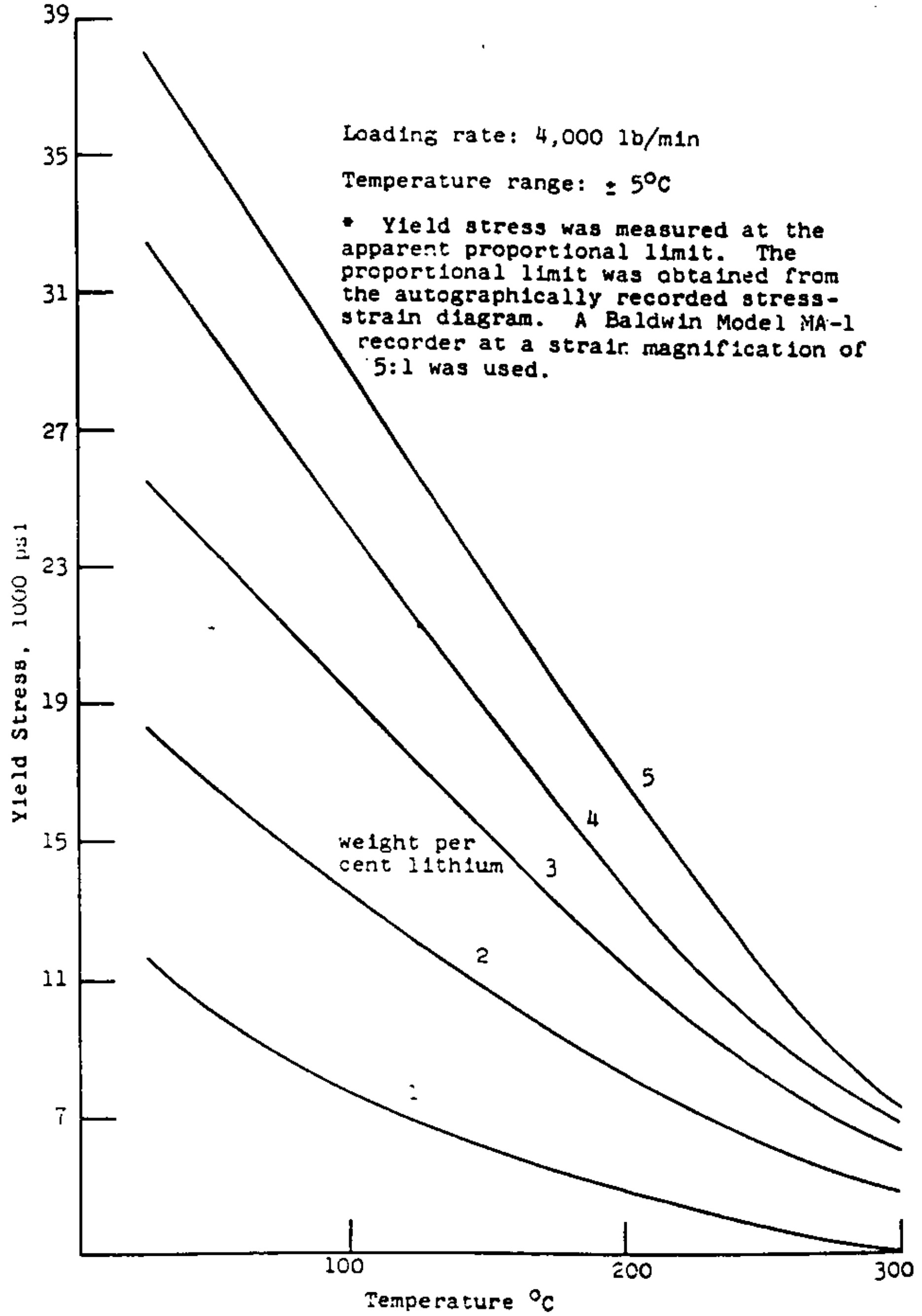

Loading rate: 4,000 lb/min

Temperature range: ± 5°C

* Yield stress was measured at the apparent proportional limit. The proportional limit was obtained from the autographically recorded stress-strain diagram. A Baldwin Model MA-1 recorder at a strain magnification of 5:1 was used.

FIGURE E4

EFFECTS OF TEMPERATURE ON HARDNESS OF ALUMINUM-LITHIUM ALLOYS

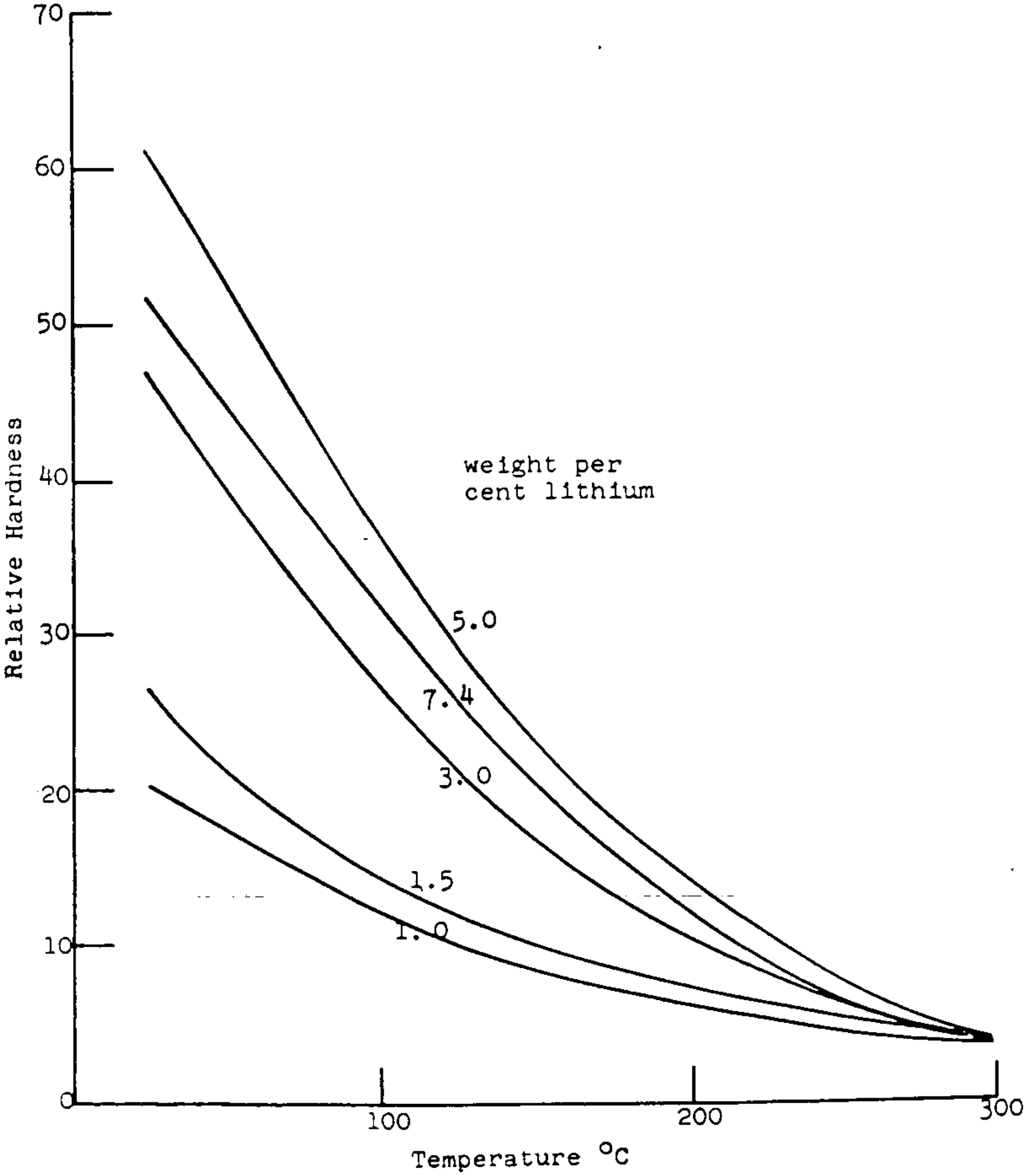

FIGURE E5

CREEP CURVES FOR AS-EXTRUDED AL-3.4 WT % LI ALLOY AT 8300 TO 8600 PSI STRESS

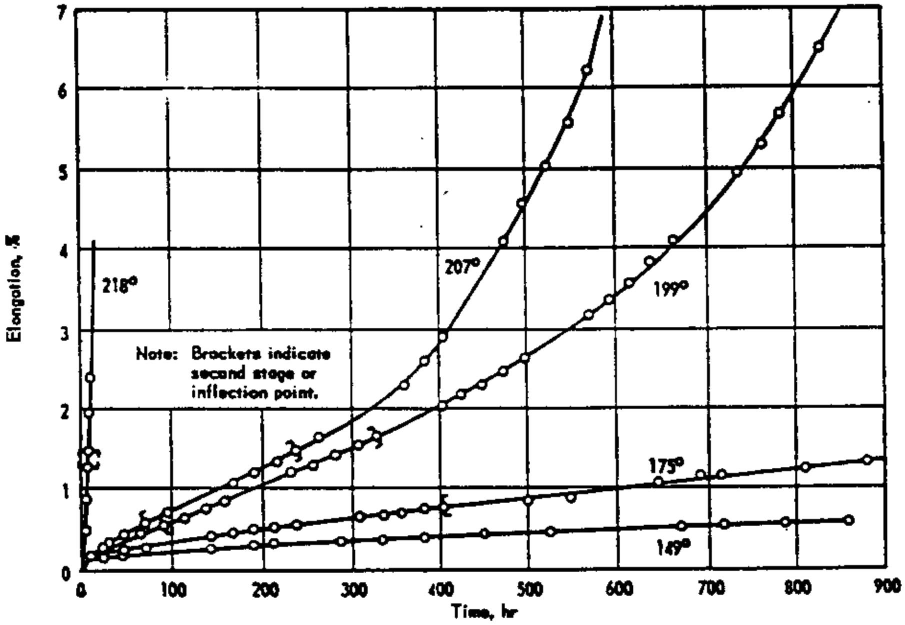

FIGURE E6

EFFECT OF TEMPERATURE ON CREEP OF AL-3.4 WT % LI ALLOY (STRESS - 8600 PSI)

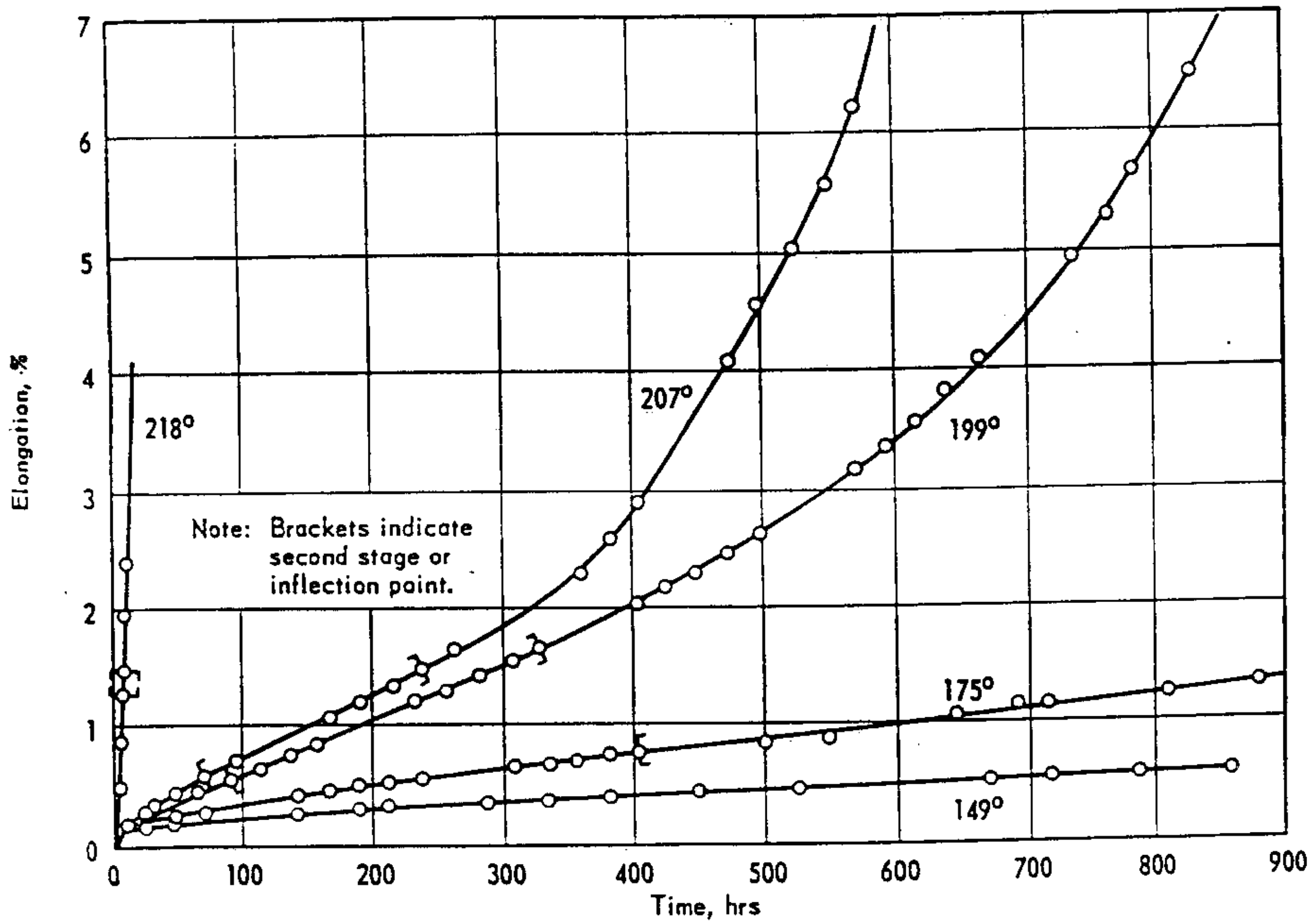

FIGURE E7

EFFECTS OF TEMPERATURE ON MINIMUM CREEP RATE OF AL-3.4 WT % LI ALLOY

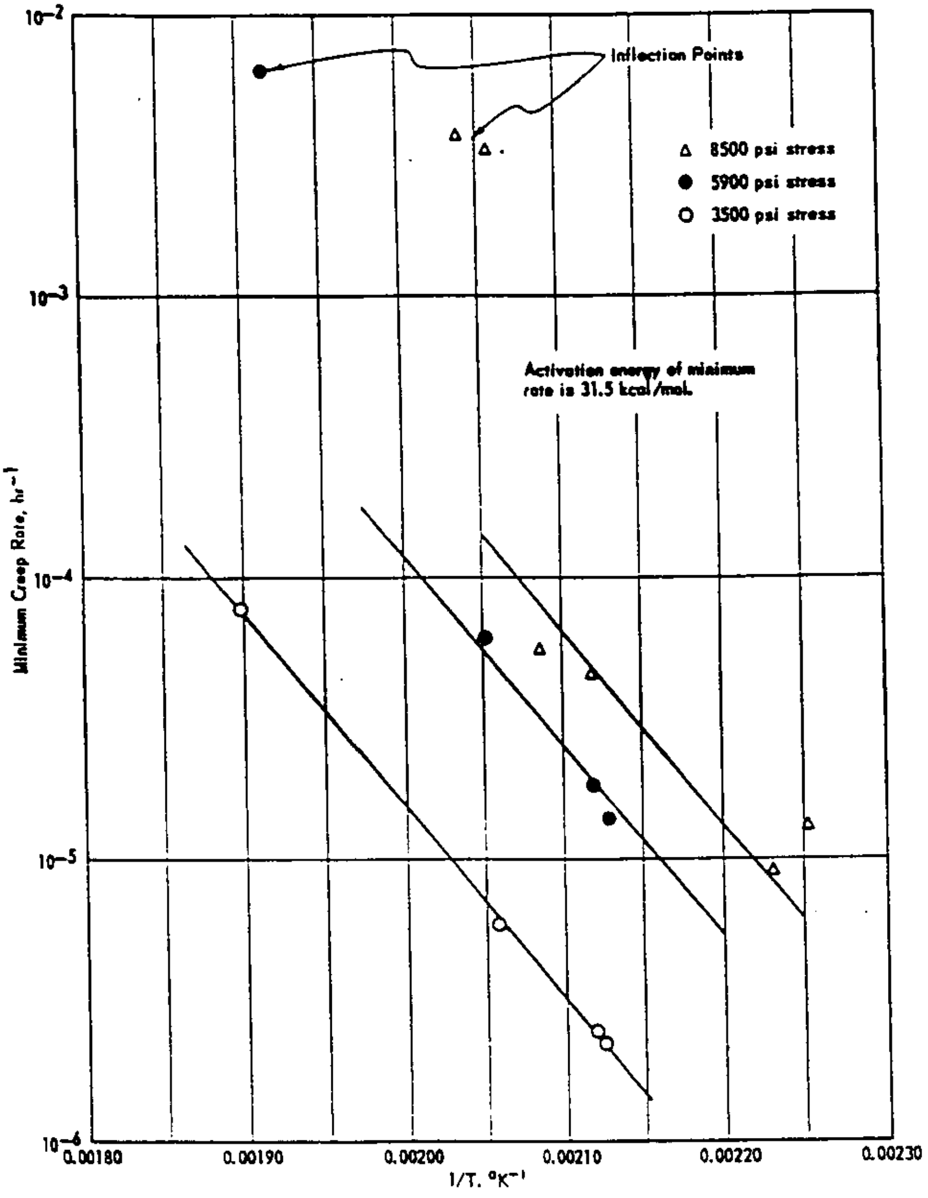

FIGURE E8

EFFECTS OF STRESS ON TEMPERATURE - COMPENSATED MINIMUM CREEP RATE

The linearity of the plot of log $\dot{E}e^{H/RT} = n \log \sigma + \log B$ indicates that the minimum creep rate $\dot{E}$ varies with stress σ as σ^n. Slope of line, n, in plot is 3.5.

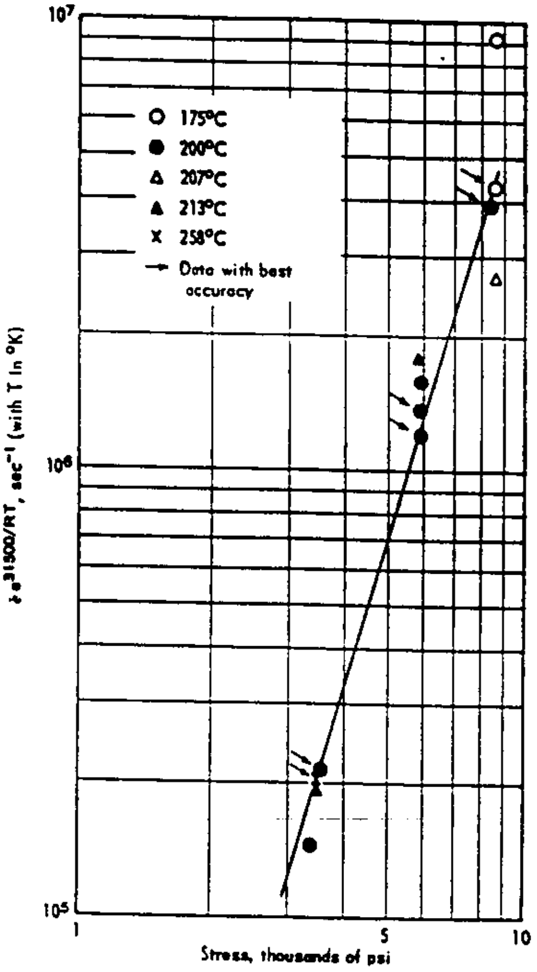

F. Irradiation Behavior[15]

Tritium and Helium Distributions[16-21]

Newly formed tritium, with a range 30-45 μm, is initially distributed throughout both α(Al) and β(LiAl) phases, but reacts with LiAl on moderate heating (150-375°C), in accord with the following reaction:

$$LiAl + T \underset{>400^\circ C}{\overset{<375^\circ C}{\rightleftarrows}} LiT + Al$$

Newly formed helium with a range about 5 μm, on the other hand, remains in the α-phase near β-phase particles, and on heating tends to collect in α-phase or interface gas bubbles. Tritium and helium distributions are summarized in Tables F1 and F2. The α-phase of a 7.4% Li alloy initially contains more tritium (81%) than expected on basis of its volume fraction in the alloy (53%). After heat treatment, most of the tritium is contained in the β-phase. The time dependence of α-phase diffusion of tritium to combine with β-phase LiAl (Figure F1) indicates a first order reaction with $K=2.35 \times 10^4 \exp(-2.00 \times 10^4/RT)$.[21] The α-phase helium content, initially 70-90% of total, is also diminished by heat treatment.

Reaction of tritium with β-phase LiAl promotes retention of the tritium in target elements at low temperatures during irradiation, and governs the kinetics of the recovery process at high temperatures following irradiation. Equilibrium decomposition pressures for lithium hydrides (H, D, & T) are much greater in the presence of aluminum than for the hydrides alone (Table F3 and Figure F2). For the decomposition reaction

$$LiT + Al \rightarrow LiAl + 1/2\, T_2$$

the equilibrium pressures of tritium are 300 to 600 times the pressures for thermal decomposition of pure LiT. Hydrogen pressure-concentration isotherms for 3.2 and 1.2 wt % Li alloys show a dependence of equilibrium hydrogen pressure on the hydrogen content (GVR) of the system Figures F3 and F4.[23] The temperature dependence of the equilibrium constant (Table F4, Figure F5)

$$K = a_{LiAl}\, a_{H_2}^{0.5} / a_{LiH}\, a_{Al}$$

is defined by the equation

$$\ln K = -\Delta H/RT + \Delta S/R$$

where $\Delta H = 14.9 \pm 0.4$ K cal mole $^{-1}$
and $\Delta S = 14.5 \pm 0.6$ K cal mole $^{-1}$ deg $^{-1}$

TABLE F1

DISTRIBUTION OF TRITIUM AND HELIUM IN IRRADIATED AL-LI ALLOY

Wt % Li in Alloy	Chips from Slug No.	Heat Treatment Time (hr)	Heat Treatment Temp°C	Fraction of β-Phase Dissolved by CH3OH (%)	Fraction of Total Tritium in α Phase (%)[a]	Fraction of Total Helium in α Phase (%)
7.4	1	None		79.6	71.9	83
	1	None		78.2	84.4	89
	2	None		70.4	85.5	72
	2	None		76.2	83.4	76
	2	1	200[b]	77.3	0.0	37
	2	1	300[b]	79.2	0.0	44
	1	4	375[c]	74.5	0.0	74
	1	4	375[c]	70.6	3.5	-
	1	4	375[c]	73.4	3.8	59
3.5	3	None		16.0	25	81
	4	None		15.5	73	93
	4	None		16.7	84	90
	4	1	300[b]	28.7	40	66

[a] Corrected for incomplete dissolution in β phase by CH_3OH.

[b] Chips heat-treated after machining.

[c] Slug heat-treated before machining.

TABLE F2

DISTRIBUTION OF TRITIUM IN IRRADIATED 7.4 WT % LI ALLOY

Heat Treatment of Wafers Time (hr)	 Temp (°C)	Fraction of Total Tritium in a Phase of Chips Machined from Wafers after Heat Treatment (%)
None		80
0.25	300	61
0.25	300	60
1.0	300	23
1.0	200	69
2.0	200	60
8.0	150	80
64	150	66
64	150	64
144	150	65

FIGURE F1

TIME DEPENDENCE OF α PHASE TRITIUM IN HEAT TREATED 7.4 WT % LI ALLOY

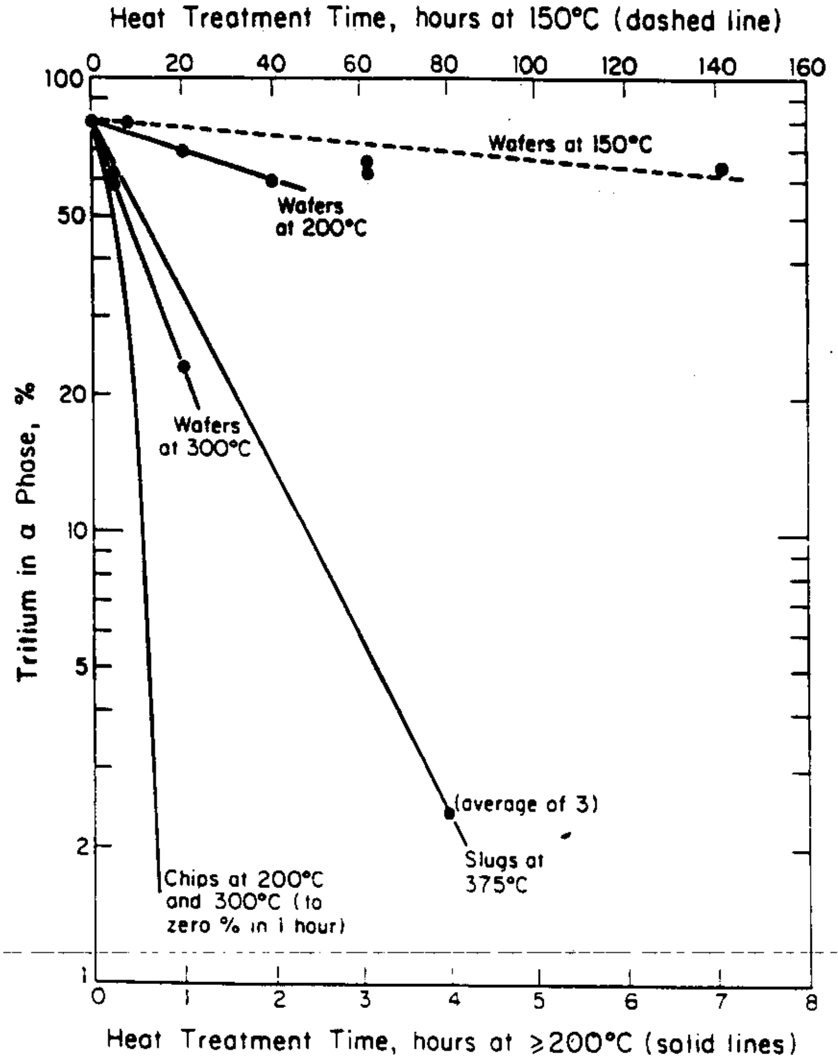

TABLE F3

EQUILIBRIUM PRESSURES OF LITHIUM HYDRIDES FOR HYDROGEN, DEUTERIUM, AND TRITIUM

Gas	In Contact With	Temp (°C)	Press (mm)	Gas	In Contact With	Temp (°C)	Press (mm)
H_2	LiH/Al[a]	247	12	D_2	LiD/Al[a]	147	1
		258	15			178	2
		287	19			190	3
		296	21			206	3
		304	24			214	4
		342	54			215	4
		347	40			222	5
		360	44			231	6
		382	27			253	8
		384	60			275	14
		423	58			304	34
		424	134			354	44
		448	84			398	66
		466	181			415	71
		500	258			461	117
		501	248			492	212
		502	408			506	289
		510	477[b]			534	433
		534	496[b]				
		548	478	T_2	Li-Al[c]	400	31
		558	497			450	123
		583	432			475	196
		586	552			500	297
						525	438
						550	588
						575	769

[a] Prepared by thermal decomposition of $LiAlH_4$, $LiAlD_4$ at 200°C,[9] e.g., $LiAlH4 \rightarrow LiH + Al + 3/2H_2$.

[b] For unirradiated 3.5 wt % Li alloy, not LiH.

[c] Irradiated 3.5 wt % Li alloy.

FIGURE F2

EQUILIBRIUM PRESSURES OF HYDROGEN ISOTOPES FOR THE DECOMPOSITION OF LITHIUM HYDRIDES WITH AND WITHOUT ALUMINUM

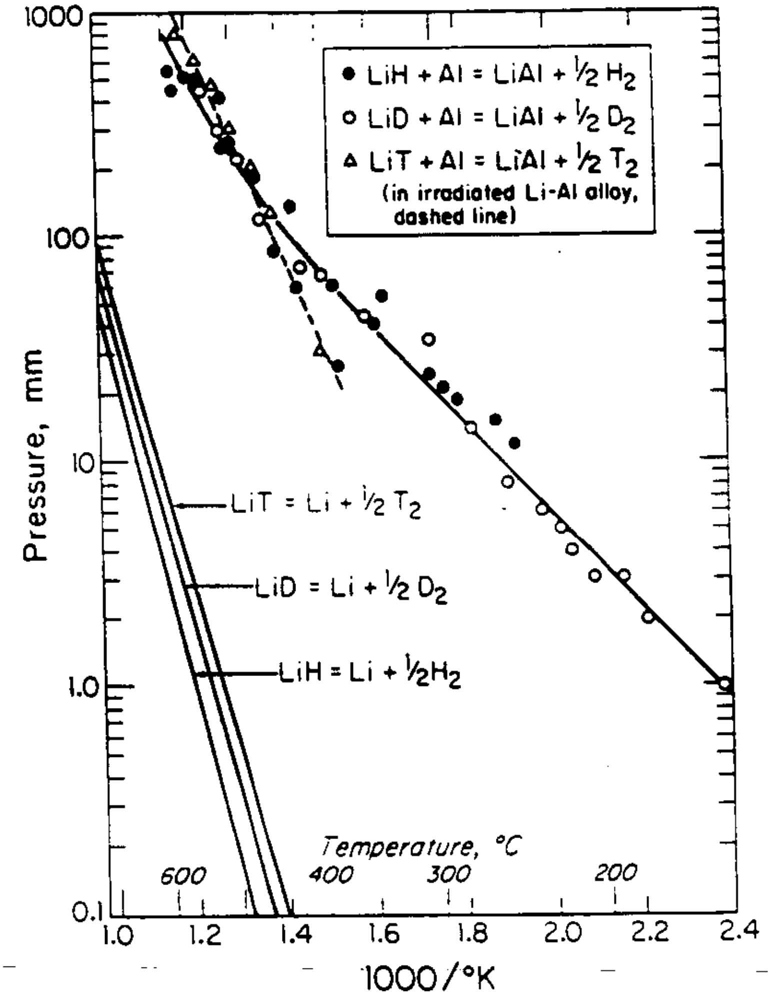

TABLE F4

EQUILIBRIUM CONSTANTS FOR THE REACTION $LiH + Al \rightarrow LiAl + 1/2H_2$

Wt % Li in Alloy	Temp (°C)	1000/T(°K)	GVR (cm^3 H_2/cm^3 alloy)	P_{H_2}[a] (mm)	$\sqrt{P_{H_2}}$ (atm)$^{1/2}$	a_{LiAl}	a_{Al} = 1 - a_{LiAl}	K
3.2	375	1.543	2.5	10	0.1147	0.1260	0.8740	0.0165
			5	11	0.1203	0.1234	0.8766	0.0169
			10	12	0.1257	0.1184	0.8816	0.0169
			20	15	0.1405	0.1082	0.8918	0.0171
			30	18	0.1539	0.0981	0.9019	0.0167
			40	22	0.1701	0.0880	0.9120	0.0164
			50	27	0.1885	0.0779	0.9221	0.0159
			60	32	0.2052	0.0678	0.9322	0.0149
			70	49	0.2539	0.0577	0.9423	0.0155
			80	89	0.3422	0.0476	0.9524	0.0171
	475	1.337	2	143	0.4338	0.1265	0.8735	0.0628
			5	160	0.4588	0.1234	0.8766	0.0646
			10	175	0.4799	0.1184	0.8816	0.0644
			20	230	0.5501	0.1082	0.8918	0.0668
			30	295	0.6230	0.0981	0.9019	0.0678
			40	380	0.7071	0.0880	0.9120	0.0682
			50	500	0.8111	0.0779	0.9221	0.0685
			60	640	0.9177	0.0678	0.9322	0.0667
1.2	325	1.672	6	6	0.0889	0.0425	0.9575	0.0039
			10	9	0.1088	0.0378	0.9622	0.0043
			20	23	0.1740	0.0283	0.9717	0.0051
			30	67	0.2969	0.0189	0.9811	0.0057
			40	240	0.5620	0.0094	0.9906	0.0053
	375	1.543	5	52	0.2616	0.0425	0.9575	0.0016
			10	80	0.3244	0.0378	0.9622	0.0127
			20	180	0.4867	0.0283	0.9717	0.0142
			25	270	0.5960	0.0236	0.9764	0.0144
	395	1.497	5	140	0.4292	0.0425	0.9575	0.0191
			10	200	0.5130	0.0378	0.9622	0.0201
	460	1.364	1	530	0.8351	0.0463	0.9537	0.0405
			3	710	0.9665	0.0444	0.9556	0.9449

[a] Hydrogen pressures corresponding to specified GVR's were read from Figures F3 and F4.

FIGURE F3

HYDROGEN PRESSURE-CONCENTRATION ISOTHERMS FOR 3.2 WT % LI ALLOY

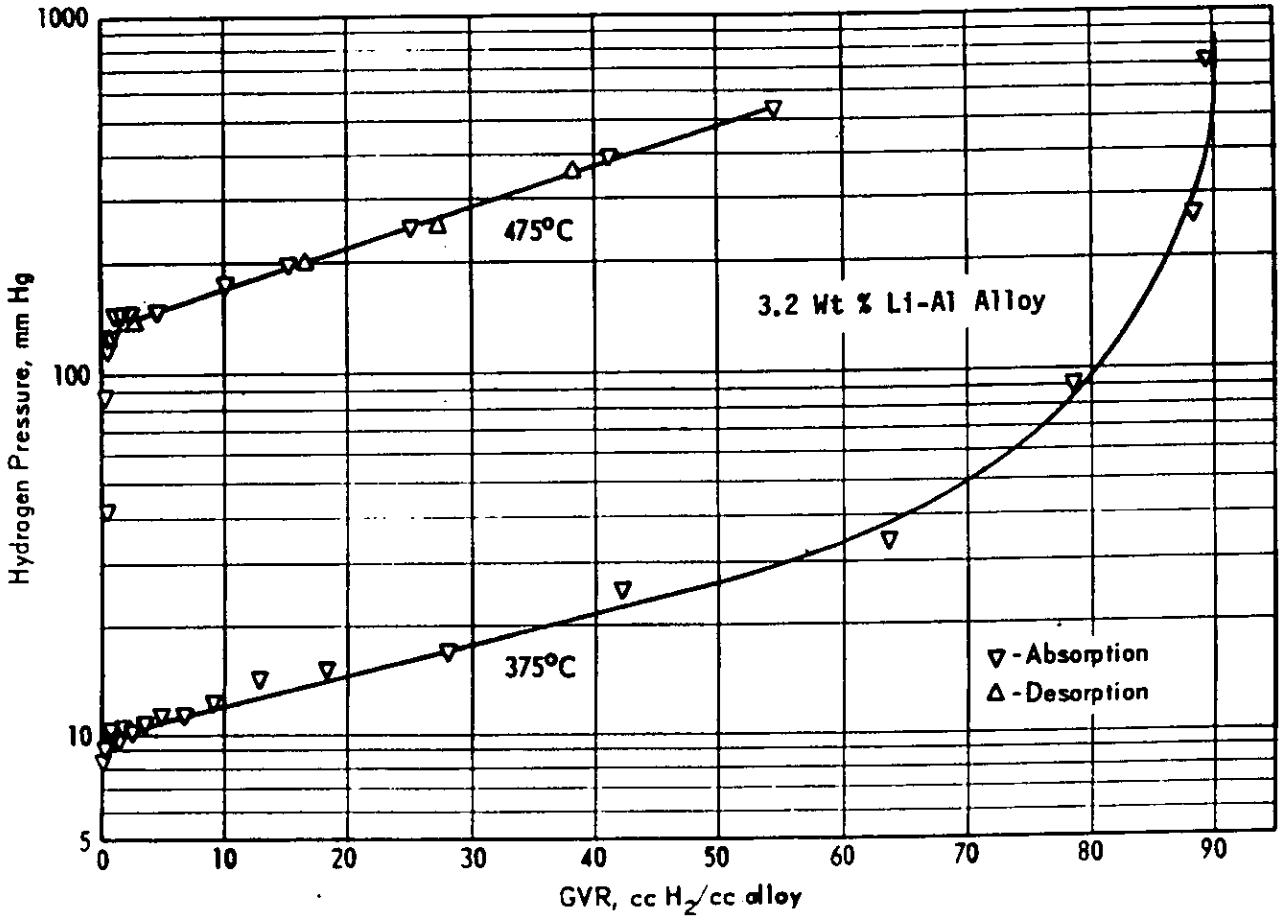

FIGURE F4

HYDROGEN PRESSURE-CONCENTRATION ISOTHERMS FOR 1.2 WT % LI ALLOY

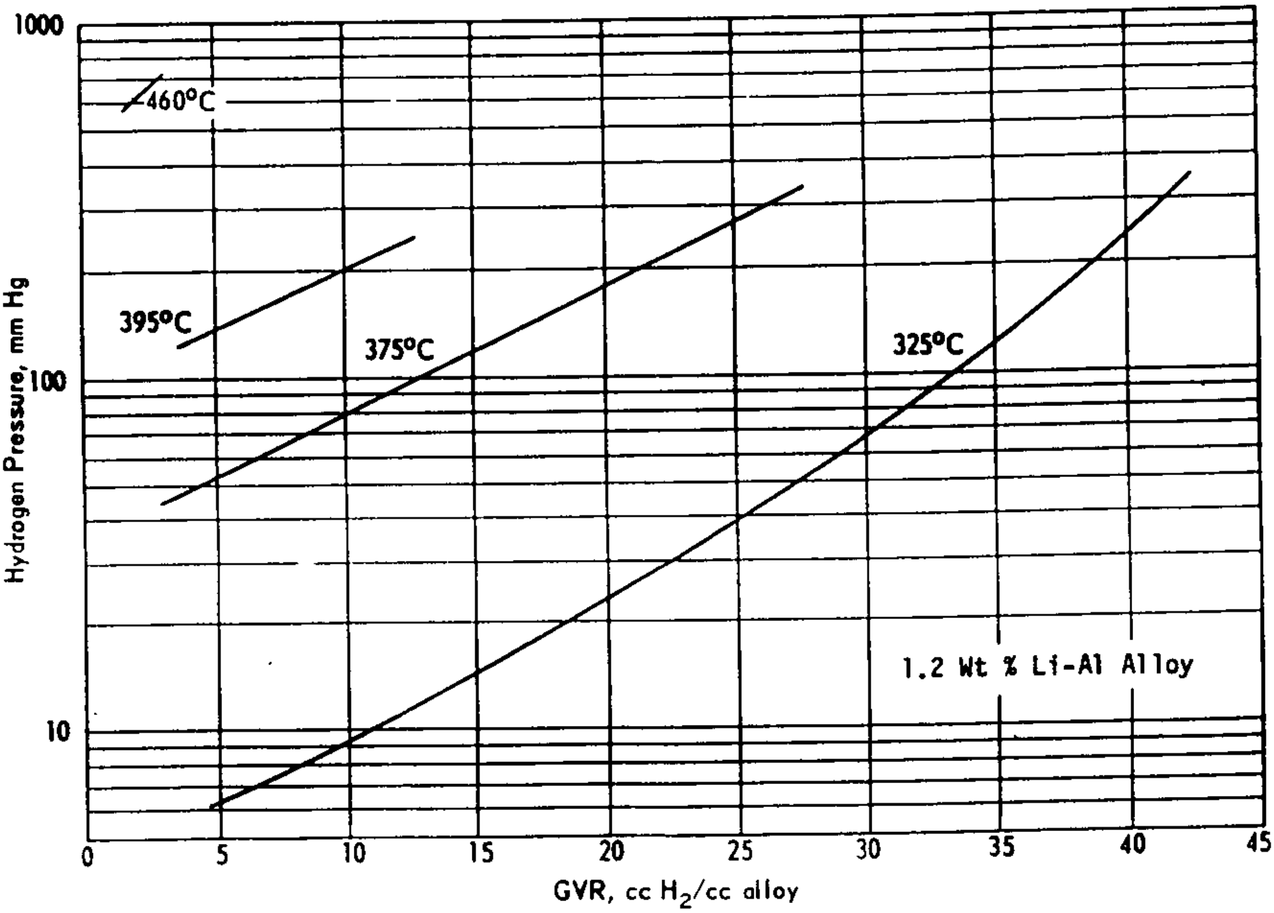

FIGURE F5

TEMPERATURE DEPENDENCE OF THE EQUILIBRIUM CONSTANT FOR THE REACTION LiH + Al → LiAl + 1/2 H_2

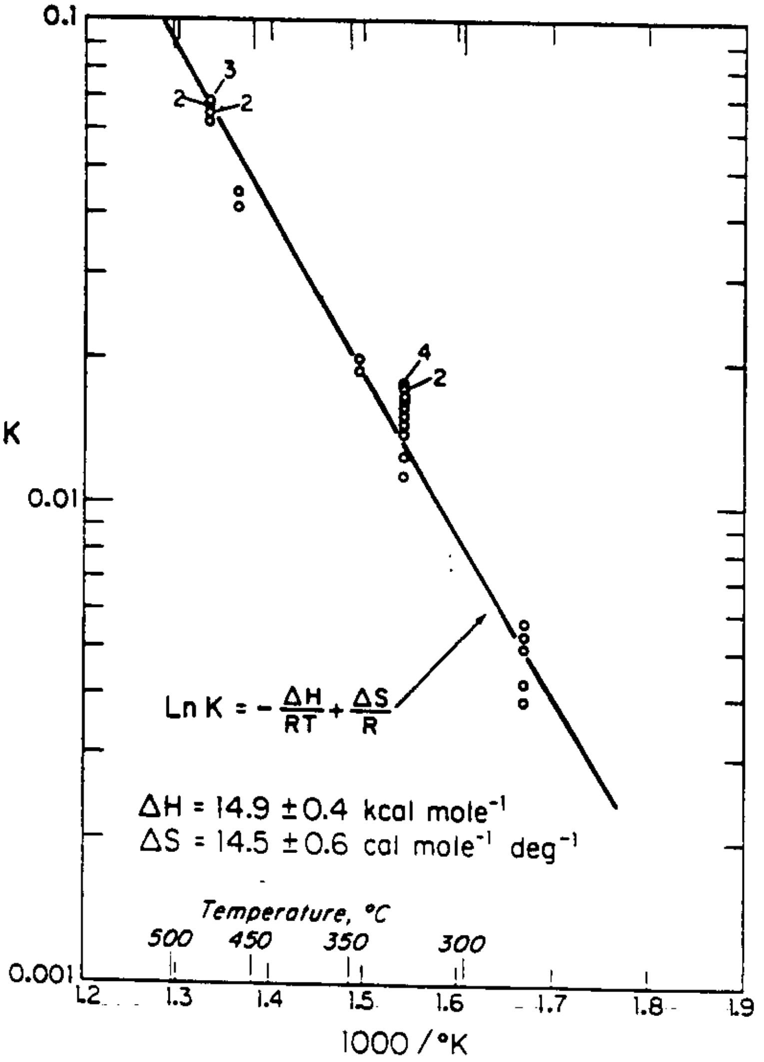

Swelling and Gas Release

Exposure limits for Al-Li target irradiations are governed by swelling and gas release thresholds.[23,24] Exposures during normal SRS reactor operation are restricted to less than 130 GVR for alloys in which the generated tritium does not exceed residual lithium concentrations (allowing complete reaction of tritium with LiAl).[25] In practice, the residual Li concentrations are maintained by restriction on Li-6 enrichment to less than 50%.

Due to the reaction of tritium with β-phase LiAl in the target elements, swelling under irradiation is attributed mainly to effects of helium generation. Low temperature irradiations at less than specified exposure limits produce very little swelling, but serve to harden and embrittle the alloys.[26,27] Temperature thresholds for swelling of helium generating materials during irradiation and post-irradiation heating generally decrease with increasing exposure (Figure F6).[28] For Al-Li alloys, the swelling thresholds approach ambient reactor temperatures near the specified exposure limits (130 GVR). Temperature thresholds for significant tritium release during product recovery operations occur at considerably higher temperatures (375-500°C).[29]

Microstructural effects of initial heat treatment also affect swelling behavior and gas release.[30] As-extruded specimens containing Li contents above 2.5 wt % expand preferentially in radial directions by a ratio of 5/1 (Table F5). Solution quenching 2.5 to 3.5 wt % Li alloy specimens from 550°C increases gas release thresholds 50°C compared to the as-extruded alloy; resultant swelling of the solution quenched specimens is greater overall, but less anistropic and more crack resistant than that of the as-extruded alloy. No effect of prior heat treatment on swelling behavior of alloys containing less than 1-2 wt % lithium (below solubility limits) is observed.

FIGURE F6

EFFECT OF INTERNAL He GENERATION ON PROPERTIES OF METALS

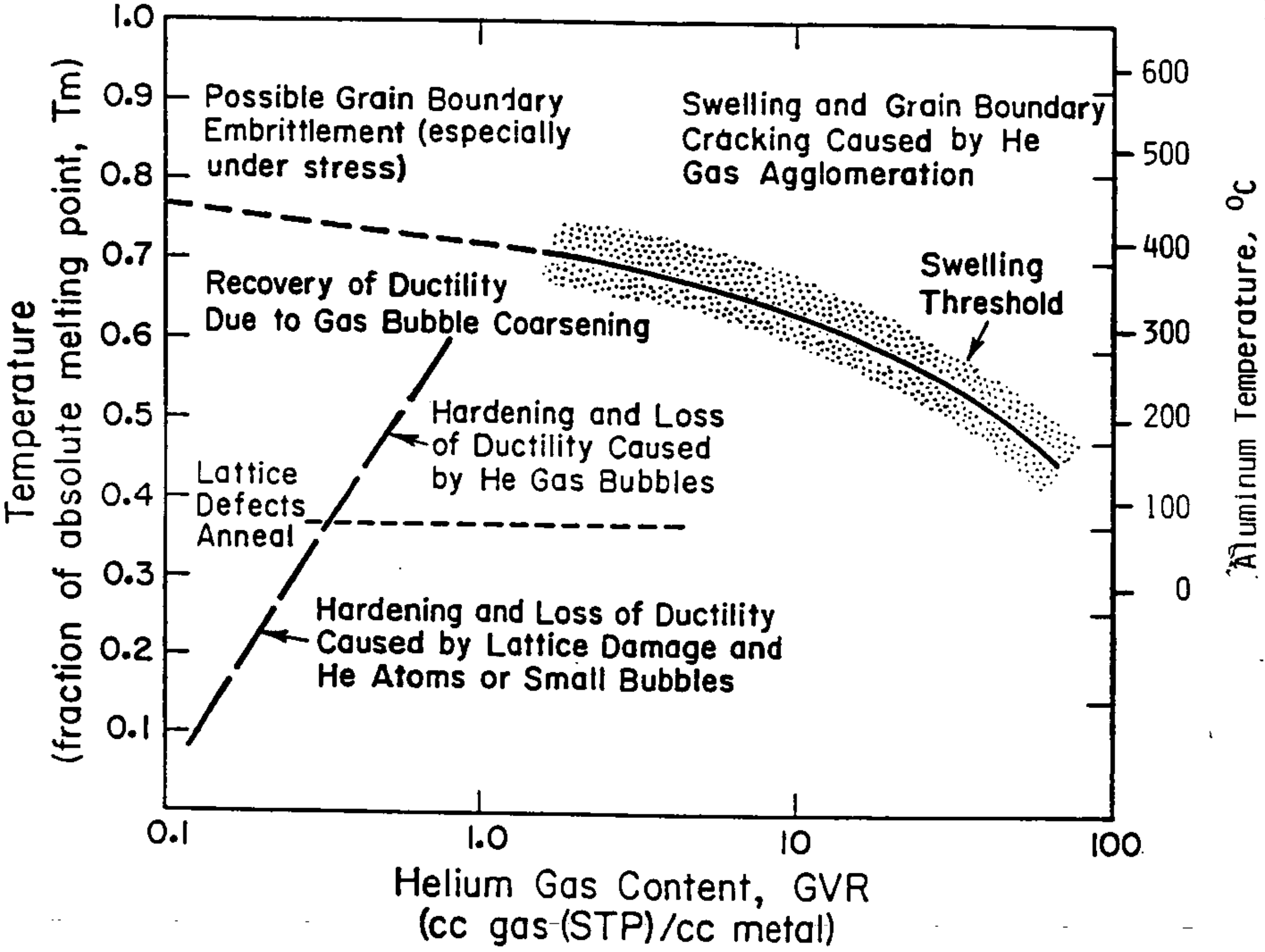

TABLE F5

DIRECTIONAL EXPANSION DURING GAS RELEASE

Sample Shape	W/O Li	Fabrication Condition	GVR	Extraction Temp. °C	Extraction Time, Hr	Expansion Radial[a]	Expansion Long[a]	Rad./Long Ratio
Square	3.5	Extruded	30	475	6.0	25	5	5.0
Slab	3.5	Extruded	30	475	6.0	31	6	5.2
Cylinder	2.6	Extruded	71	488	2.0	32	48	6.7
Cylinder	2.6	Annealed	73	495	6.5	44	28	1.6
Cube	1.6	Extruded	57	495	3.5	12	10	1.2
Cube	1.7	Annealed	55	495	4.0	14	11	1.3

---

[a] Radial is perpendicular to original extrusion direction; longitudinal is parallel to original extrusion direction.

B. Annealed 3 hr at 440°C, quenched (solution treatment).

Gas Release Process

Tritium release during product recovery is promoted by target swelling and cracking due to helium agglomeration.[31,32] Measurements of specimen expansion and gas release during isothermal product extractions demonstrate specimen swelling and helium release prior to collection of the major fraction of tritium recovered (Figure F7).[33] The mechanism of tritium release is presumed to involve interconnection of helium gas bubbles to comminute the target structure, allowing recovery of tritium released by the aluminum promoted decomposition of LiT.

The magnitude of swelling during product recovery operation is characterized by the following equation

$$\ln V = -\frac{9360}{T} + 0.92 \ln G + 1.24L + 10.20$$

where V = % vol increase
T = temperature for 2-6 hours, °K (range 350-600°C)
G = gas volume ratio total helium and tritium (range 2.4 to 92)
L = wt % Li in alloy after irradiation (range 1.1 to 2.7)

Gas release kinetics are as follows:

(a) for tritium $$\frac{-dQ_1}{dt} = K_1Q_1, \quad \log K_1 = \frac{-31{,}000}{T} + 3.5 \log G_{He} + 36.75$$

where t = time (min), K_1 = tritium release coeff (min^{-1}), Q_1 = residual tritium (cc) and G_{He} = gas volume ratio initial helium.

(b) for helium $$\frac{-dQ_2}{dt} = K_2Q_2^2, \quad \log K_2 = \frac{-42{,}100}{T} + 4.75 \log G_{He} + 47.99$$

where K_2 = helium release coefficient (min^{-1}), and Q_2 = residual He (cc He/cc alloy)

Expansion pressures produced by heating during product recovery operations of restrained specimens (3.5% alloy exposed to 31 GVR) were observed to increase from 1000 psi at 380°C to over 6000 psi at 510°C (Figure F8 and F9). Circumferential restraint forces expansion accompanying product release into longitudual directions (Figure F10). Totally restrained expansion inhibits tritium and helium release during product recovery operations.

FIGURE F7

CHRONOLOGY OF ISOTHERMAL EXTRACTIONS

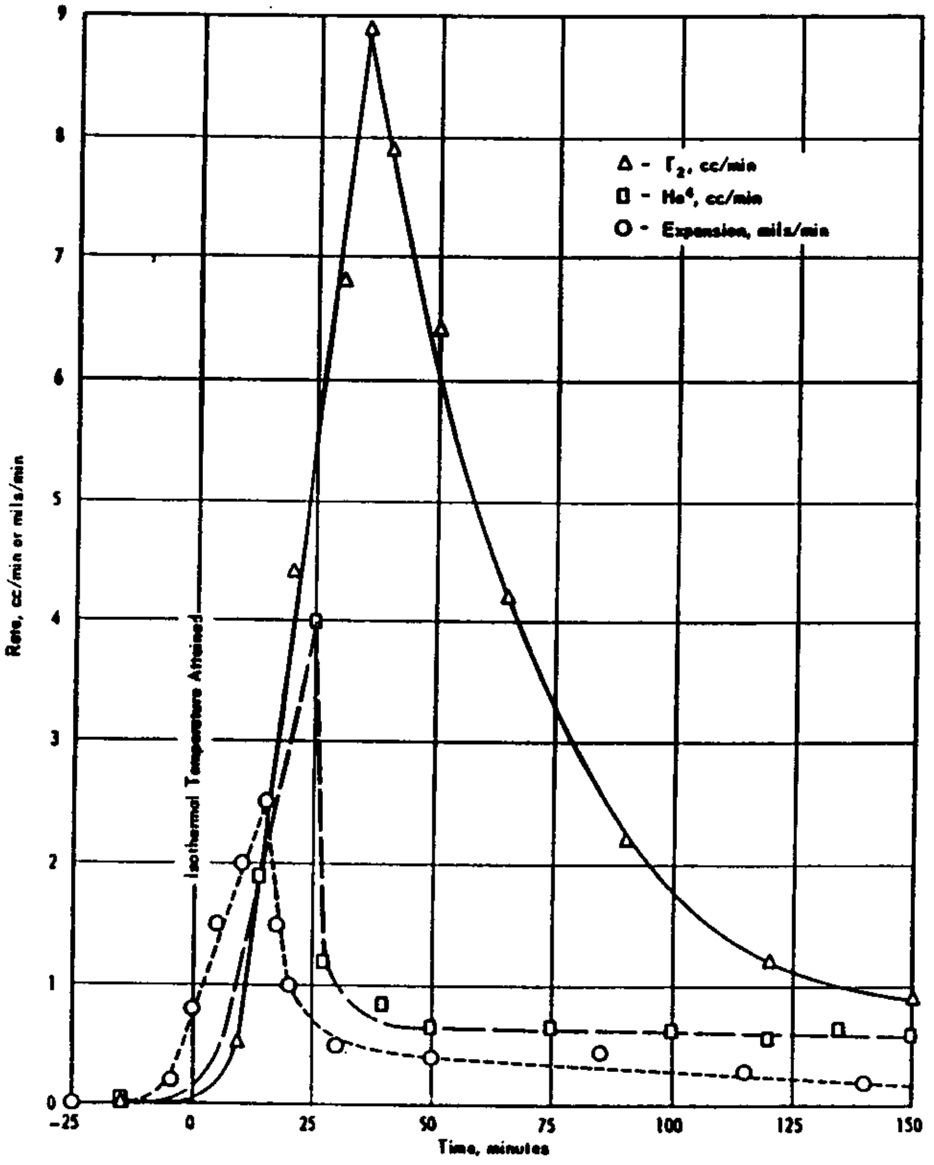

FIGURE F8

EXPANSION PRESSURE MEASURING DEVICE

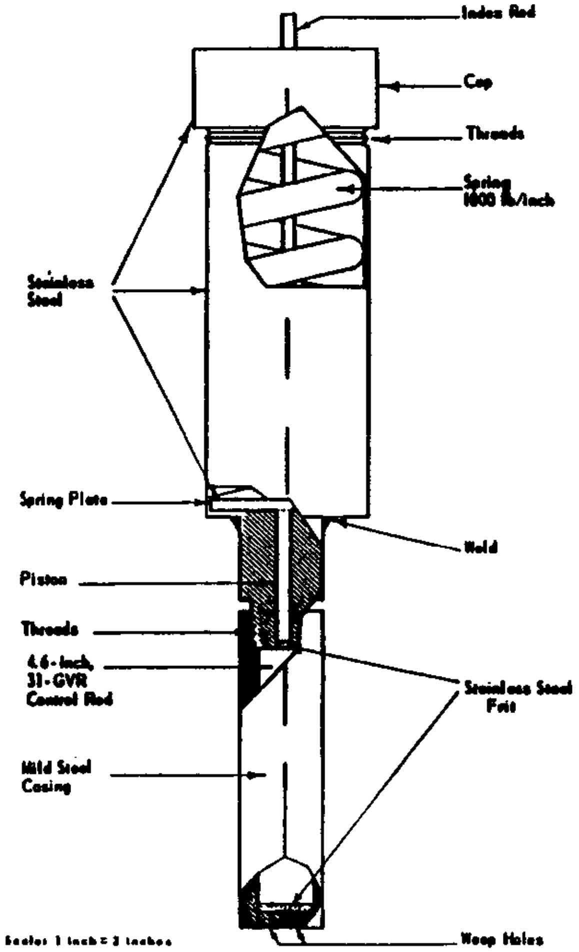

FIGURE F9

TEMPERATURE DEPENDENCE OF EXPANSION PRESSURE

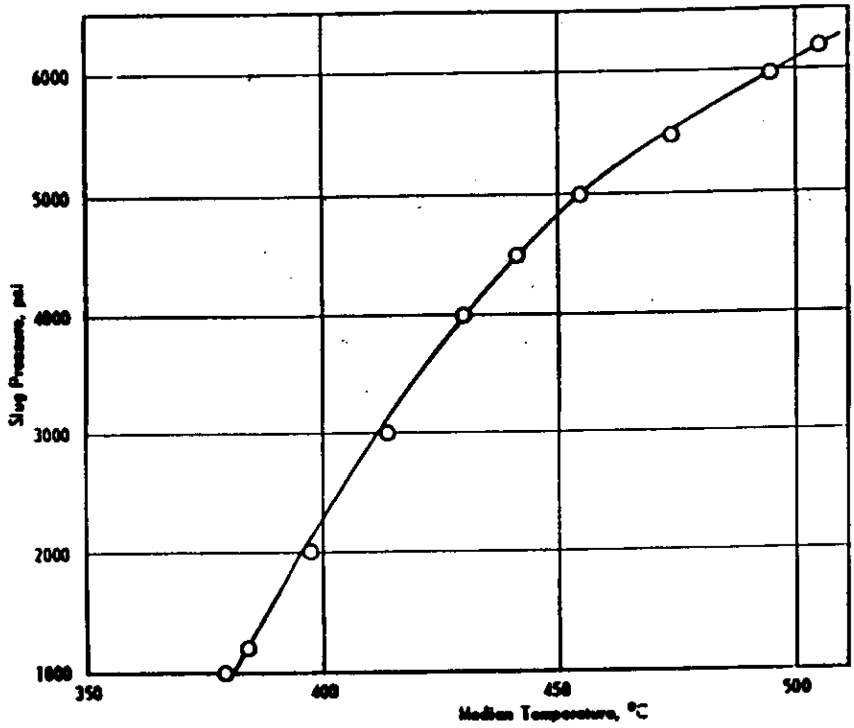

FIGURE F10

FORCED LONGITUDINAL EXPANSION

Results of 30 hours at 496°C for 3-3/4 inches of 8.7 GVR, 3.5%, natural lithium target element encased in a 5-inch steel cylinder.

REFERENCES

1. L. H. Meyer, "Tritium", Kirk-Othmer Encyclopedia of Chemical Technology, A. Standen, ed, Vol C, 2nd Ed., John Wiley and Sons, Inc., New York, 910 (1965)
2. Metals Handbook, 8th Ed, Metallography, Structures, and Phase Diagrams, Am. Soc. for Metals, 1973, p. 261
3. M. L. Holzworth, Aluminum Lithium Alloys, DPST-60-446, Aug. 15, 1960 (Secret).
4. C. L. Angerman, Aging of Al-Li Alloys - Part 1, DP-331, January 1959 (Secret).
5. L. P. Costas and R. P. Marshall, "The Solubility of Lithium in Aluminum", Trans Met Soc AIME, 224, 970 (1962) (DPST-61-499, Nov. 8, 1961)
6. R. P. Marshall and L. P. Costas, The Solubility of Lithium in Aluminum, DPST-61-183, Feb. 28, 1961.
7. L. P. Costas, Thermal Conductivity of Aluminum-Lithium Alloys Containing Up to 8% Lithium, DP-463, April 1960.
8. L. P. Costas, The Diffusion of Lithium in Aluminum, DP-813, Feb. 1963.
9. R. P. Marshall, "Strain-Induced Diffusion and Precipitation in Aluminum-Lithium Alloys During Creep," Acta Metallurgica, 9, 958 (1961) (DPST-61-209, Feb. 28, 1961).
10. L. P. Costas, Thermal Migration of Lithium in Aluminum Lithium Alloys, DP-540, Jan. 1961 (Secret).
11. R. P. Marshall, Physical Metallurgy and Irradiation Behavior of Aluminum-Lithium Alloy, DPST-61-470 Rev., Nov. 1961 (Confidential)
12. R. P. Marshall, Deformation of Aluminum-Lithium Alloys During Irradiation, DP-547, Feb. 1961 (Secret).
13. V. I. Montenyohl, Physical and Mechanical Properties of Al-Li, DPST-60-319, May 31, 1960.
14. R. P. Marshall, Creep of Aluminum-Lithium Alloy, DP-622, October 1961 (Confidential).
15. W. R. McDonell and C. L. Angerman, Irradiation Behavior of Al-Li Alloys, DPST-82-1018, Nov. 17, 1982 (Secret).
16. J. H. Owen and D. Randall, "Equilibrium and Kinetic Studies of Systems of Hydrogen Isotopes, Lithium Hydrides, Aluminum, and $LiAlO_2$," Radiation Effects and Tritium Technology for Fusion Reactors (International Conference Gatlinburg, TN, Oct. 1-3, 1975) CONF-750989, Vol III, p 433.

17. L. H. Meyer and M. O. Fulda, Mode of Retention of Gases in Irradiated Li-Al Alloy.I-Distribution of Tritium and Helium Between Alpha and Beta Phases, DP-378, May 1959.

18. L. H. Meyer and M. O. Fulda, Mode of Retention of Gases in Irradiated Li-Al Alloy.II-Reaction Between Lithium Tritide and Aluminum, DP-397, July 1959.

19. F. G. Rust, Mode of Retention of Gases in Irradiated Li-Al Alloy.III-Gas Released by Mechanical Subdivision, DP-501, August 1960 (Secret).

20. M. O. Fulda and L. H. Meyer, Mode of Retention of Gases in Irradiated LiAl Alloy.IV-Species of Tritium Evolved During Aqueous Dissolutions, DP-529, Nov. 1960 (Secret).

21. M. O. Fulda and L. H. Meyer, Mode of Retention of Gases in Irradiated Li-Al Alloy.VI-Kinetics of the Migration of Tritium, DP-530, Nov. 1960 (Secret).

22. D. W. Tharin, Jr., Equilibrium Pressure of Hydrogen Over Li-Al Alloy, DP-791, Feb. 1963 (Secret).

23. I. M. Macafee, Irradiation Performance of Lithium Targets, DPST-66-384, May 20, 1966 (Secret).

24. J. H. Owen, Effects of Lithium Concentration and Li/T Atom Ratio on Tritium Release from Irradiated Li-Al, DP-891, June 1964 (Secret).

25. 105-Building Technical Standards, DPSTS-105--2.10 (4/1/75) E. I. du Pont de Nemours and Company, September 1988.

26. R. P. Marshall, Irradiation of Aluminum-Lithium Alloy Slugs, DP-332, Feb. 1959 (Secret).

27. C. L. Angerman, R. P. Marshall and T. O. Williams, Irradiation and Annealing of Al-Li Slugs, DP-424, Dec. 1959 (Secret).

28. W. R. McDonell and W. C. Mosley, "Long-Term Integrity of ^{252}Cf Source Materials" Proc. Topical Meeting on Applications of Californium-252, Austin, Texas, Sept. 1972, CONF-720502, 61 (1972); W. R. McDonell, "Temperature Thresholds for Surface Blistering of Platinum and Stainless Steel Exposed to ^{242}Cm Alpha Radiations, "Trans Am. Nucl. Soc., 39, 442 (1981).

29. D. W. Tharin, Jr., Extraction Threshold in Irradiated Li-Al Alloy, DP-633, Sept. 1961 (Secret).

30. D. W. Tharin, Jr., Increased Dimensional Stability for Li-Al Targets, DP-590, June 1961 (Secret).

31. F. G. Rust, Mode of Retention of Gas in Irradiated Li-Al Alloy.V-Distribution of Gas and Porosity During Extraction, DP-637, Oct. 1961 (Secret).

32. D. W. Tharin, Jr., Expansion of Irradiated Li-Al Alloy, DP-744, Oct. 1962 (Secret).

33. D. W. Tharin, Jr., Kinetic of Gas Extraction from Irradiated Li-Al Alloy, DP-743, Dec., 1962 (Secret).